Impact of Relative Intensity Noise on 60-GHz Radio-Over-Fiber Wireless Transmission Systems

Hamza Hallak Elwan, Ramin Khayatzadeh, Julien Poette, Beatrice Cabon

Impact of Relative Intensity Noise on 60 GHz Radio-over-Fiber Wireless Transmission Systems

Hamza Hallak Elwan, Ramin Khayatzadeh, Julien Poette, and Beatrice Cabon

***Abstract*—This paper investigates a 60 GHz radio-over-fiber (RoF) communication system employing two different techniques to generate millimeter-wave (mm-wave) signals. The relative intensity noise (RIN) transferred during optical heterodyning of mm-wave signal is theoretically studied and experimentally investigated. Laser RIN induces noise at resultant electrical mm-wave signal and is directly generated from initial RIN at low frequency. Therefore, RIN impairs the performance of the RoF mm-wave system. The model of RIN is also presented and is in very close agreement with the experiment results. Furthermore, wireless transmission experiments to demonstrate the intensity noise effect are carried out and are compliant with the standards at mm-wave. Wireless transmission up to 3 m can be achieved using a transmit power of +4.5 dBm.**

***Index Terms*—Error vector magnitude (EVM), distributed feedback (DFB) laser, millimeter-wave (mm-wave), passively mode locked laser diode (PMLLD), phase noise, radio-over-fiber (RoF), relative intensity noise (RIN).**

I. Introduction

FUTURE wireless applications demand a large sufficient bandwidth to satisfy greater data rates [1]. Millimeter-wave (mm-wave) frequency band and beyond has been proposed as a solution to overcome the saturation of spectral resources [2]. The unlicensed frequency band of 7 GHz from 57 to 64 GHz is allocated for wireless communications which rapidly expands 60 GHz technology for ultra-high speed systems [3]. The huge attenuation of the atmosphere and the electronic challenge of solid state signal source in this continuous frequency band emerge wireless propagation difficulties [4]-[6]. Therefore, microwave photonic technologies have intensely been proposed for mm-wave signal generation, and radio-over-fiber (RoF) has been utilized to distribute mm-wave signals [7],[8]. The optical signals carrying data are transmitted from the central station (CS) to the base station (BS) by an optical fiber. Optical modes can be mixed on a high-speed photodiode (PD) at the BS to generate mm-wave signal, and heterodyning advantage is that mode beating avoids any external electrical oscillator [9], for example by beating two independent running lasers [8]. In this approach, the resultant signal exhibits a large phase noise induced by laser linewidth, wavelength fluctuations and mode correlation [10]. Then, monolithic dual distributed feedback (DFB) lasers are developed for obtaining a narrow linewidth beat note with reduced phase noise [11]. Another approach uses quantum dash mode-locked laser (QD-MLL) to demonstrate mm-wave beat note linewidth around 100 KHz [9].

Relative intensity noise (RIN) of laser is an indicator of the laser intensity stability and is usually measured from DC to some GHz in [12]. For mm-wave RoF communication systems, RIN has been explored in [13], and the impact of intensity noise on generated mm-wave signals has be observed on error vector magnitude (EVM) [14]-[16]. The photonic mm-wave generation with low phase noise is used by optical carrier suppression (OCS) or optical modulator, but the high insertion loss is experienced and the large RF drive power is required. Thus, in this paper, we demonstrate the RIN effect close to the mm-wave carrier using two techniques for optical heterodyne generation with low and high phase noise values of mm-wave signal. The Erbium-doped fiber amplifier (EDFA) is not implemented to avoid the amplified spontaneous emission (ASE) noise. The first technique uses two independent distributed feedback (DFB) lasers without any locking scheme which is the simplest and cheapest way. In this case, phase noise is larger than in other solutions and its measurement is presented using the technique in [17] to de-correlate RIN and phase noise impacts on resultant mm-wave signal. The second technique is based on a passively mode-locked laser diode (PMLLD) at 60.64 GHz to generate mm-wave signal with advantage of lower phase noise due to the correlation between optical modes of the PMLLD. At the receiver-end, a coherent receiver using a mixer is used for electrical down-conversion. Both theoretical and experimental studies confirm that the RIN phenomenon in mm-wave frequency band is generated from the initial RIN at low frequency. It is worth mentioning that the results of the presented study are applicable to any kind of optical frequency generation. Depending on the heterodyne process, it is shown that RIN at mm-wave signal can be larger than the initial RIN at low frequency and causes spectral degradation in optical heterodyne signals.

The results presented in [13] are extended to examine the impact of intensity noise on EVM for 60 GHz RoF wireless system using 60 GHz antennas and envelop detector (ED) as incoherent receiver. Data rates of 397 Mbps and 794 Mbps with binary phase shifting keying (BPSK) modulation format are applied as well as a data rate of 1588 Mbps with quadrature phase shifting keying (QPSK) modulation format to comply with communication standards at 60 GHz [18],[19].

This paper is organized as follows: section II investigates the theory and experimental setup of RIN. In section III, experimental measurements of RIN are analyzed in [9 KHz-19 GHz] and in [50-62] GHz frequency ranges. A 60 GHz RoF wireless system is discussed in section IV, and finally the

The authors are with Institut de Microélectronique Electromagnétisme et Photonique - LAboratoire d'Hyperfréquences et de Caractérisation, IMEP-LAHC, Minatec, 3 Parvis Louis Néel CS 50257 38016 Grenoble Cedex 1, France e-mail: (hamza.hallak-elwan@imep.grenoble-inp.fr).

conclusion is presented in section V.

II. Theoretical Investigation and Experimental Setup of RIN

Generating mm-wave signal by optical heterodyning requires at least two optical signals. The optical field $E_i(t)$ can be expressed as:

$$E_i(t) = A_i\big(1+\delta_i(t)\big)\exp\Big(j\big(2\pi f_i t + \phi_i(t)\big)\Big) \quad (1)$$

where A_i, δ_i, f_i, and ϕ_i are the amplitude, amplitude noise, frequency, and phase noise of the optical field of mode (i), respectively. For each laser, RIN expression was described in [20], and for a standard semiconductor laser, the generic expression of RIN that can be extracted from laser rate equations is:

$$RIN_i(\omega) = \frac{\big\langle|\delta_{opt}(\omega)|^2\big\rangle}{\langle P_{opt}\rangle^2} = \frac{PSD(\omega)}{P_{elec}} = 4\delta_i^2(\omega) \quad (2)$$

where $\delta_{opt}(\omega)$ is the optical power variation spectrum, P_{opt} is the optical power, *PSD* is the power spectral density of the intensity noise, P_{elec} is DC electrical power, and $\delta_i(\omega) = FFT\left(\delta_i(t)\right)$.

A. RIN Generated by Two DFB Lasers

The generic schematic diagram of experimental setup for two separate optical sources (first technique) is shown in Fig. 1. Two independent DFB lasers, DFB_1 and DFB_2 operating in the C-band, are used to generate a beat note carrier which is adjusted and controlled by the temperature and the bias current of the two lasers. The polarization controller (PC) is utilized for optimizing the beating power, and a (50/50) coupler is used to mix the two optical signals on a PD of 70 GHz bandwidth.

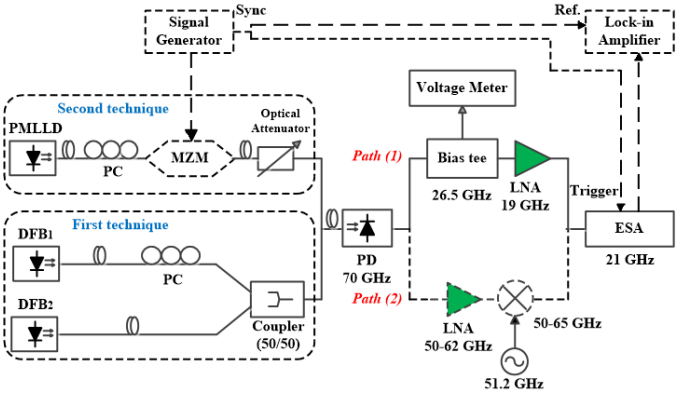

Fig. 1. Experimental setup for optical heterodyning based on two independent lasers or PMLLD in [9 KHz-19 GHz] and [50-62] GHz.

The combined signal after a coupler is transmitted through a conventional single mode optical fiber of 1.5 m length to a high-speed PD at the receiver-end. In this case, the beating results from only two modes which are not phase locked, and consequently the fiber length will just impact on the received optical power. The photodetected current $I_{PD}(t)$ is expressed as:

$$\begin{aligned} I_{PD}(t) = {} & (I_1+I_2) + \Big(I_1\sqrt{RIN_1(t)} + I_2\sqrt{RIN_2(t)}\Big) \\ & + 2\sqrt{I_1 I_2}\times\cos\Big(2\pi(f_2-f_1)t + \big(\phi_2(t)-\phi_1(t)\big)\Big) \\ & + \sqrt{I_1 I_2}\Big(\sqrt{RIN_1(t)} + \sqrt{RIN_2(t)}\Big) \\ & \times\cos\Big(2\pi(f_2-f_1)t + \big(\phi_2(t)-\phi_1(t)\big)\Big) \end{aligned} \quad (3)$$

where I_i is the DC photodetected current of the optical signal ($i,\ i=1\ or\ 2$), and RIN_i is relative intensity noise $RIN(t) = FFT^{-1}(RIN(\omega))$. Second order terms related to noise-to-noise beatings have been neglected.

The first term of (3) represents the total average current, the second term represents the noise current of two optical signals from DC to some GHz corresponding to the initial relative intensity noise (RIN_{ini}), the third term is the beat note current created during their simultaneous detection where the beat frequency is equal to difference between frequencies of the two optical modes (f_2-f_1), and the last term represents noise current of the two optical signals corresponding to RIN close to beat note (RIN_{beat}). The frequency (f_2-f_1) exhibits a phase noise $(\phi_2(t)-\phi_1(t))$ which amplitude varies due to the correlation between these modes, that depends on how the two optical modes are produced. In the last term of (3), it can be noticed that RIN amplitude at beat note depends on the product of modes amplitudes in opposition to RIN amplitude at low frequency represented by the second term. This nonlinear process at beat note could lead to an increase of intensity noise during heterodyne process with respect to initial intensity noise at low frequency. This increase is noticeable especially when the optical powers of the two lasers are different.

After substituting (3) in (2), and as there is no correlation between modes when considering two independent DFB lasers, the auto-correlation function of $RIN_1(t)$ and $RIN_2(t)$ is equal to 0. Therefore, the (RIN_{ini}) at low frequency and (RIN_{beat}) close to the beat signal are then obtained as follows:

$$RIN_{ini}(f) = \frac{I_1^2 RIN_1(f) + I_2^2 RIN_2(f)}{(I_1+I_2)^2} \quad (4)$$

$$RIN_{beat}(f) = \frac{I_1 I_2\big(RIN_1(f)+RIN_2(f)\big)}{(I_1+I_2)^2} \quad (5)$$

As can be seen in the last term of (3), the product of the mode intensity noise and the carrier in the time domain leads to the intensity noise conversion in the frequency domain directly to the beat frequency. In case the optical signals have the same amplitudes $(I_1 = I_2)$, then $RIN_{ini} = RIN_{beat}$. While a power difference exists, for example $(I_2 > I_1)$, the RIN_i of the less powerful mode (RIN_1) in this case, is increased by a factor I_2/I_1 in (5) as compared to RIN_i in (4), and thus, RIN_{beat} is larger than RIN_{ini} by a factor I_2/I_1. This phenomenon has not been published by other authors to the best of our knowledge and is evidenced in section III with both experimental and model results.

For more accurate recognition between RIN_{ini} and RIN_{beat}, and for avoiding down-conversion stage, we first present

results in [9 kHz-19 GHz] frequency band. For measuring RIN in [9 KHz-19 GHz] frequency range, path 1 of Fig. 1 is used. After PD, a bias tee is added to suppress the DC component and to extract the photocurrent value for RIN determination. A 19 GHz low noise amplifier (LNA) having a 40 dB gain is employed. For analyzing RIN in the mm-wave frequency band, path 2 is implemented, and therefore the mm-wave signal is amplified using a 35 dB gain LNA of (50-62) GHz bandwidth. Then, the amplified signal is down-converted by using a mixer (50-65) GHz of 6 dB losses and a local oscillator (LO). Finally, an electrical spectrum analyzer (ESA) of 21 GHz bandwidth is monitored to extract power spectral density (PSD) of measured RIN.

B. RIN Generated by PMLLD

The optical field $E(t)$ of any multi-mode laser i.e., PMLLD, possessing (M) modes equally spaced can be defined as:

$$E(t)=\sum_{i=1}^{M} A_i\big(1+\delta_i(t)\big)\exp\Big(j\big(2\pi\big(f_0+if_r\big)t+\phi_i(t)\big)\Big) \quad (6)$$

where A_i, δ_i, and ϕ_i are the amplitude, amplitude noise, and phase noise of i^{th} mode, respectively. f_0 and f_{RF} are the frequency of the first mode and the beat note frequency which corresponds to the free spectral range (FSR). Fig. 1 shows the generic schematic diagram of experimental setup based on PMLLD (second technique) for two frequency bands. In some cases, the sensitivity of the system can be improved using a lock-in amplifier to measure the intensity noise [12]. A digital signal generator drives a Mach-Zehnder modulator (MZM), and a synchronization is necessary between ESA and lock-in amplifier. The output current of the PD $I_{PD}(t)$ can be described as:

$$\begin{aligned} I_{PD}(t) = &\sum_{i=1}^{M} I_i + \sum_{i=1}^{M} I_i\sqrt{RIN_i(t)} \\ &+ 2\sum_{i,j:i\neq j}\sqrt{I_iI_j}\times\cos\Big(2\pi(f_j-f_i)t+\big(\phi_j(t)- \\ &\phi_i(t)\big)\Big)+\sum_{i,j:i\neq j}\sqrt{I_iI_j}\left(\sqrt{RIN_i(t)}+\sqrt{RIN_j(t)}\right) \\ &\times\cos\Big(2\pi(f_j-f_i)t+\big(\phi_j(t)-\phi_i(t)\big)\Big) \end{aligned} \quad (7)$$

The RIN_{ini} at low frequency and RIN_{beat} at fundamental beat note can be expressed as:

$$RIN_{ini}(f)=\left(\frac{\sum_{i=1}^{M}\left(I_i\sqrt{RIN_i(f)}\right)}{\sum_{i=1}^{M} I_i}\right)^2 \quad (8)$$

$$RIN_{beat}(f)=\left(\frac{\sum_{i=1}^{M-1}\left(\sqrt{I_iI_{i+1}}\left(\sqrt{RIN_i(f)}+\sqrt{RIN_{i+1}(f)}\right)\right)}{\sum_{i=1}^{M} I_i}\right)^2 \quad (9)$$

All beating noise expressed in the last term of (7) which are not used in (9) contribute on noise at other frequencies corresponding to harmonics of the beat note. Equations (4) and (5) can be seen as specific cases of equations (8) and (9) when only 2 modes are considered. Terms of (7) for (M) modes have the same expressions as terms in (3) for two modes. RIN expressions of (8) and (9) are also the same as (4) and (5) respectively. The main and important difference between the two mm-wave generation techniques cases is the correlation between modes is not considered null for the case using PMLLD.

III. Experimental Measurements of RIN

The RIN results are here measured in [9 KHz-19 GHz] frequency band as well as in [50-62] GHz.

A. Experimental Results in [9 KHz-19 GHz] Frequency Band

The fundamental features of the technique using two different DFB lasers (Fig. 1 - path 1) are the ability to generate beat signals at different frequencies and the capability to demonstrate several cases of RIN close to beat note by varying the temperature and the relative optical power of the DFB lasers. Due to the relaxation frequency of the lasers of 4.1 GHz and the 19 GHz bandwidth limitation of the amplifier, a beat signal at 14 GHz has been chosen to highlight the impact of RIN in optical heterodyne process as shown on Fig. 2.

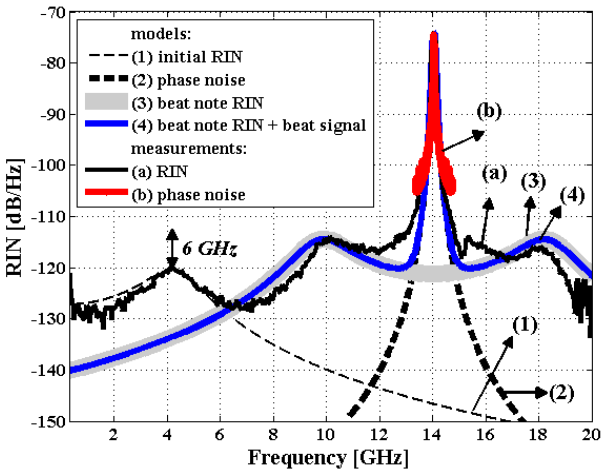

Fig. 2. RIN and phase noise of a heterodyne signal at 14 GHz for generation using two independent DFB lasers.

For verifying (4) and (5), the bias current of the first laser DFB_1 is set to 15 mA (P_{opt}= -2.1 dBm) while the bias current of the second laser DFB_2 is 90 mA (P_{opt}= +3.5 dBm). Thus, RIN_1 and RIN_2 levels are very different for the first and second laser, respectively. The experimental results of initial RIN_{ini} and beat note RIN_{beat} are given in curve (a) of Fig. 2. On these results, the thermal noise impact, the shot noise and the frequency response of the global system have been removed. In Fig. 2, the initial RIN_{ini} from 9 KHz to 7 GHz and RIN close to the generated beat note RIN_{beat} on each side of the heterodyne signal can be observed. The large phase noise obtained by this technique is provided in curve (b) to prove that impairments are not due to phase noise but come from laser intensity noise

solely. The beat note linewidth is estimated to be 30 MHz in this case. From (4) and (5), the difference between the maximal values of initial noise RIN_{ini} and noise close to the beat note RIN_{beat} is calculated to be equal to 6.7 dB. From experimental measurement of Fig. 2, it can also be observed that the beat note RIN_{beat} is higher than the initial RIN_{ini} by a factor I_2/I_1= 6 dB, which is in good agreement with the predicted value of 6.7 dB. The RIN of less powerful mode (RIN_1) in (5) is then increased by a factor I_2/I_1 compared to RIN_1 in (4) as expected.

The initial RIN_{ini} has been modeled, curve (1) of Fig. 2, from RIN expression of laser [20]. The phase noise of beat signal corresponds to the convolution of the two optical individual spectrums. The noise shape can be modeled by a Lorentz distribution while other random variations at the wavelength difference are considered as Gaussian fluctuations, resulting in a Voigt profile (curve (2)). The beat note RIN_{beat} model in curve (3) refers to the last term in (3), representing the phase noise of the beating signal multiplied in the time domain by the sum of the individual laser intensity noise. Then, the model results of beat signal phase noise and RIN_{beat} are summed and shown in curve (4). Based on the aforementioned, experimental results are well confirmed by model results and give an evidence of RIN generation from heterodyne process at beat note, as presented in (3), (4), and (5).

In Fig. 3, we intend to show that RIN_{beat} impairs mm-wave signal, even at high frequency. Since the relative intensity noise (RIN_1) of DFB_1 has the main contribution on the initial RIN_{ini}, two different bias currents are set for DFB_1: 13 mA (P_{opt}= -4.1 dBm) and 17 mA (P_{opt}= -0.6 dBm), respectively. The second laser DFB_2 is still biased at 90 mA (P_{opt}= +3.5 dBm).

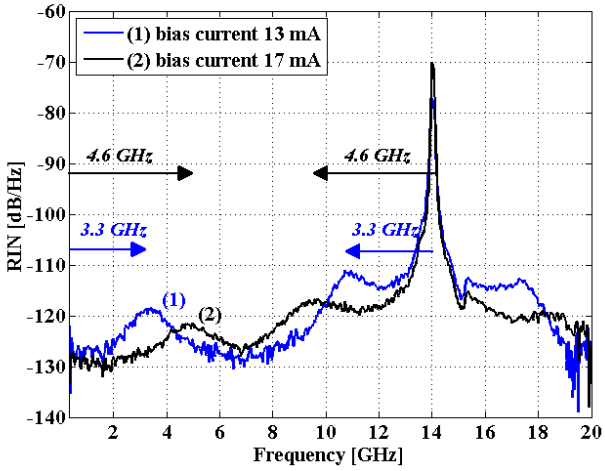

Fig. 3. RIN of the beat note at 14 GHz for two different bias currents of the first laser DFB_1.

The temperature of both lasers is set to keep the beat note at 14 GHz, and results are shown in Fig. 3. When the laser DFB_1 is biased at 13 mA, the laser relaxation frequency is equal to 3.3 GHz that can be seen on the curve (1) of Fig. 3. During the heterodyne process, it can be noted that RIN_{beat} close to the beating frequency exhibits a maximum noise at an offset from the beat note equal to the relaxation frequency. When changing the laser bias to 17 mA, the relaxation frequency is equal to 4.6 GHz (curve (2)), corresponding to the offset between the beat note and the maximum RIN_{beat}. In this case, the SNR is increased, but if the Erbium-doped fiber amplifier (EDFA) is implemented to increase the optical power, the SNR is still fixed as in Eq. (23) in [15].

From this figure, it is inferred that RIN_{beat} close to beat signal is directly generated from initial RIN_{ini} and has the same profile. The difference between initial RIN_{ini} and RIN_{beat} at beat note for the above two cases is also observed because the lowest powered mode will be increased through the heterodyne process by I_2/I_1. Fig. 3 depicts different RIN_{ini} values while keeping identical phase noise for both measurements. Then, the results clearly indicate that the beat signal for offset frequency higher than 1 GHz is largely impacted by RIN_{beat} which spread over a very large bandwidth, much higher than phase noise. This further confirms that RIN phenomenon at generated beat note is distinct from phase noise of heterodyne signal.

B. Experimental Results in [50-62] GHz Frequency Band

This subsection concerns optical mm-wave generation using 2 DFBs and PMLLD. The schematic diagram of the experimental setup is described in path 2 of Fig. 1. A mixer and an LO frequency fixed at 51.2 GHz are employed for down-conversion, to adjust received signals to the ESA bandwidth. The mixing process does not influence the quality of the involved signals as the LO phase noise is much lower than the signal to be characterized (-140 dBc/Hz for frequency offset above 10 MHz) [21].

In the first technique using 2 DFBs for mm-wave generation, the temperature of lasers is controlled to stabilize the signal at 55 GHz, and the bias current of DFB_1 is 13 mA (P_{opt}= -4.1 dBm), while the bias current of DFB_2 is set to 90 mA (P_{opt}= +3.5 dBm). Fig. 4 shows the experimental and model results, illustrating RIN_{beat} close to beat note (curve (a)) and also phase noise (curve (b)) at mm-wave frequency.

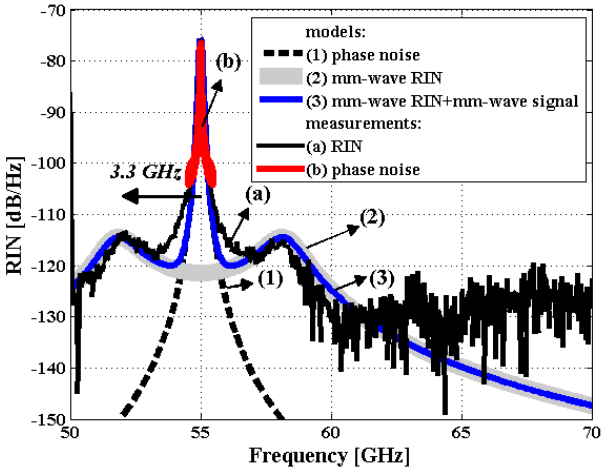

Fig. 4. RIN and phase noise of the heterodyne signal at 55 GHz with mm-wave generation based on 2 DFBs.

The models of phase noise, and RIN_{beat} in curves (1) and (2), respectively, are in very good agreement with the experimental results. The RIN_{beat} in Fig. 4 is comparably similar to the result of RIN_{beat} without down-conversion stage in Fig. 3 for bias current of 13 mA. The factor I_2/I_1 being larger than 1 as described in (4) and (5), consequently RIN_{beat} close to the beat frequency is higher than RIN_{ini} at low frequency.

In the second technique using PMLLD for mm-wave generation, PMLLD having an FSR of 60.64 GHz is biased at 180 mA (P_{opt}= +9.5 dBm), and the temperature is fixed at 25°C. Here, the lock-in amplifier allows measurements of a lower RIN level. Fig. 5 represents the beat note in [50-62] GHz range before down-conversion and only depicts one side band RIN_{beat} of mm-wave signal because of the frequency cutoff at 62 GHz. According to the correlation between optical modes of PMLLD, the beat note linewidth of mm-wave signal is $\approx$ 1 MHz, which is much lower than the first technique using 2 DFBs.

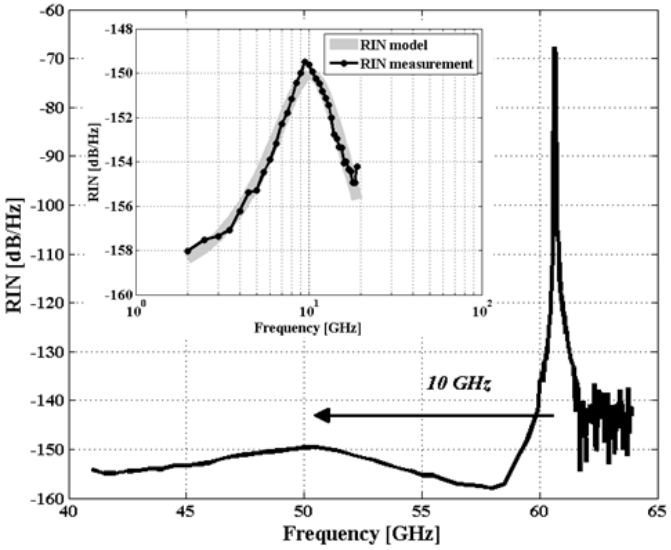

Fig. 5. RIN of the heterodyne signal at 60.64 GHz with mm-wave generation based on PMLLD.

The initial RIN_{ini} at low frequency and its model are presented in the black curve and thick grey curve in the left insert of Fig. 5, respectively. It should be mentioned that Fig.5. shows an estimation of the RIN_{beat} (black curve) at mm-wave based on low frequency measurements and using the presented model. The peak value of beat note RIN_{beat} is -150 dB/Hz at 50 GHz which is the same as RIN_{ini} peak measured at the low frequency. This can be explained by the distribution of optical power between (M) modes which are equal, thus the factor I_j/I_i equals 1 as described in (8) and (9). The relaxation frequency extracted from RIN_{ini} and RIN_{beat} is approximately 10 GHz, so it can be confirmed that RIN_{beat} is generated from RIN_{ini}. When comparing the first and second techniques, both based on same physical phenomenon, i.e. heterodyning, RIN_{beat} close to beat signal has the same origin. Since the fiber length is increased, chromatic dispersion will induce a time delay between different modes, and this can be interpreted by a de-correlation between optical modes. Consequently the noise induced by RIN will also be de-correlated. Therefore, this delay degrades the compensation of intensity noise which can not fully be compensated when detecting several modes. The frequency limit at which the compensation is possible depends on the fiber length, and the wavelength difference between beatings and the number of beatings should also be considered.

IV. 60 GHz RoF Wireless Transmission

In this section, we have studied the impact of intensity noise on broadband 60 GHz transmission complying with 60 GHz communication standards.

A. 60 GHz RoF System Setup

The experimental setup presented in Fig. 6 to perform a transmission of digital modulated data on a 60 GHz carrier in order to analyze the intensity noise impact on EVM. The central station employs the previous mentioned optical sources, 2 DFB lasers or PMLLD. A PC is added to match the polarization state of the modulator waveguide. A MZM is used as an external modulator biased at the quadrature point for applying data in compliance with standard modulation formats. Signals come from an arbitrary waveform generator (AWG), and the variable optical attenuator is employed to vary the optical power transmitted to a conventional single mode optical fiber of 1.5 meter. At the base station, the 60 GHz signal is produced by optical heterodyning on a high-speed PD and then amplified to a maximum level of +4.5 dBm using a 35 dB RF amplifier.

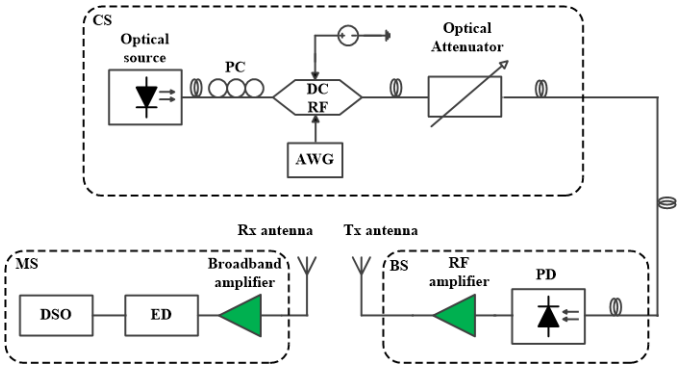

Fig. 6. Experimental setup for 60 GHz RoF wireless system based on two independent lasers or PMLLD.

Then, the wireless link is implemented by 60 GHz standard horn antennas of 20 dBi gain. A 30 dB gain broadband amplifier is used at the receiver to compensate the free space losses. The data-modulated 60 GHz signal is then recovered using ED as down-conversion stage. Since the ED only detects field intensity, the noise measured is due to the intensity noise [14],[15]. The ED does not require any LO nor locking scheme which makes this receiver cost-efficient. The down-converted signal and data are transmitted to a high-speed digital sampling oscilloscope (DSO) 54855A from Agilent, having a 6 GHz bandwidth for sampling process. On-line EVM values are obtained using vector signal analyzer (VSA) installed on the DSO.

B. Experimental Results

The EVM measurements are carried out with achieving 60 GHz communication standards for a wireless distance of 25 cm where the free space power loss is approximately 16.5 dB. This distance can be increased by using a higher transmit power and high-gain antennas. According to a bandwidth limitation of 2 GHz of the Schottky diode used, data using BPSK 397 Mbps, BPSK 794 Mbps, and QPSK 1588 Mbps modulations are applied on a 1 GHz subcarrier at 60 GHz.

For BPSK modulation using 2 DFBs or PMLLD, EVM characterizations have been performed as a function of the received RF power. BPSK 397 and 794 Mbps data rates can be shown in Fig. 7 and Fig. 8, respectively, and constellation diagrams are presented as well in inserts. The received RF power was varied by adjusting the optical power into the PD using the optical attenuator. In Fig. 7, EVM values at bit rate of 397 Mbps are as low as 10.8 % for 2 DFBs (circle points) and 11.8 % for PMLLD (square points) for the same received RF power of -20.6 dBm. The EVM value of the lowest received RF power within standard limits is defined by the receiver sensitivity. In this experiment, the values of the receiver sensitivity for 33.4 % standard limit are -42.7 dBm and -41.2 dBm for 2 DFBs and PMLLD, respectively. The wireless distance between the two antennas at these receiver sensitivity values can be extended to approximately 3 m without any additional amplifier.

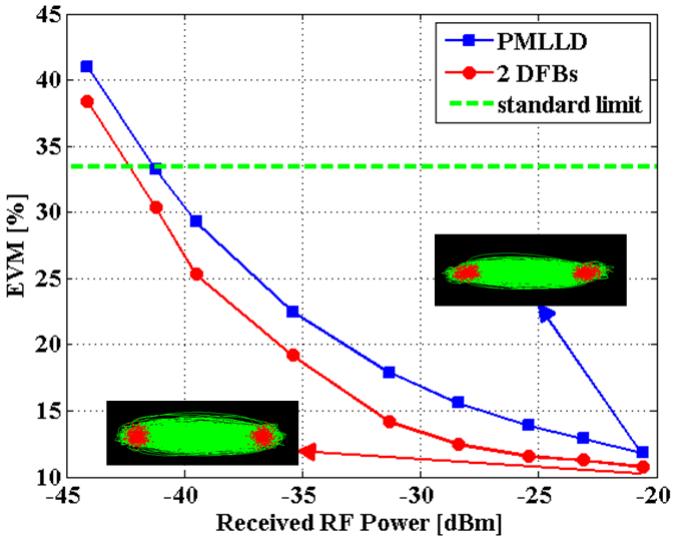

Fig. 7. EVM of the 397 Mbps BPSK signal as a function of received RF power.

As can be extracted from the constellation diagrams, the error-floors of EVM are due to the impact of intensity noise. Furthermore, the PSD measurements of the intensity noise in [15] show that the intensity noise of PMLLD is higher than 2 DFB lasers, and therefore the EVM value with PMLLD is higher than that of 2 DFBs at the same received RF power.

The EVM for a transmission of BPSK signal at data rate of 794 Mbps is illustrated in Fig. 8. The lowest EVM values achieved are 14.2 % and 15.8 % for 2 DFBs (circle points) and PMLLD (square points)at the same received RF power of

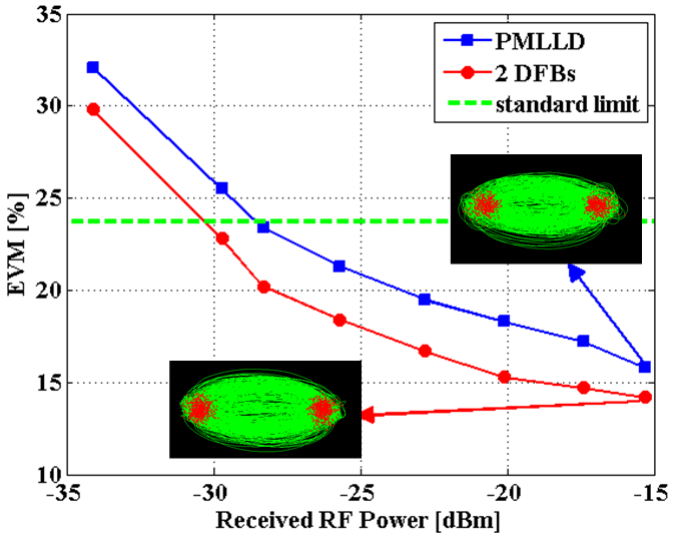

Fig. 8. EVM of the 397 and 794 Mbps BPSK signal as a function of received RF power.

-15.3 dBm, respectively. The receiver sensitivity is compliant with the standard limit of 23.7 % at -29.7 dBm for 2 DFBs and -28.3 dBm for PMLLD, while the maximum distance between two antennas at these levels of sensitivity is approximately 1.5 m, with avoiding the use of additional amplifiers. Here, since the signal bandwidth is increased, the error-floors are higher than in the case using BPSK data rate of 397 Mbps.

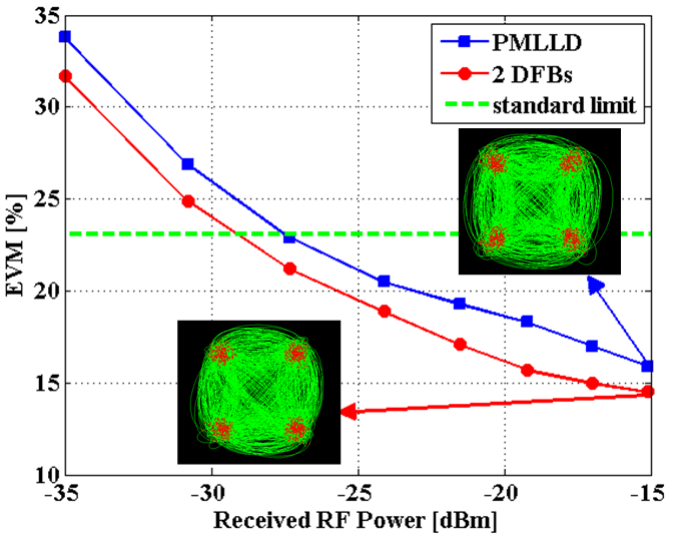

Fig. 9. EVM of the 1588 Mbps QPSK signal as a function of received RF power.

For a QPSK signal of 1588 Mbps data rate applied on the transmitter side, Fig. 9 shows the EVM trends versus received RF power. For 2 DFBs (circle points), EVM as low as 14.5 % is obtained at the received RF power of -15.1 dBm whereas for PMLLD (square points), EVM increases to 15.9 % at the same received RF power. For the standard limit of 23.1 %, the receiver sensitivity is -29.3 dBm and -27.3 dBm for 2 DFBs and PMLLD, respectively. At these values of receiver sensitivity, the transmission distance can be extended

to approximately 1.5 m with no other amplifier implemented. The constellation diagrams of QPSK modulation show that there is no phase noise impact measurable, and thus the EVM error-floors are induced by the intensity noise solely.

Finally, for reflecting the ambiguity noise in the system, BER can be calculated in [reference], and after the calculations are performed, the phase ambiguity does not influence in the system. The previous three modulation format used match the requirements of the communication standards for 60 GHz RoF wireless transmission, using 2 DFBs or PMLLD.

V. Conclusion

This paper analyzes the RIN of optical heterodyne generated signals for mm-wave RoF applications and systems. A complete theoretical study and experimental measurements have been presented using two different techniques, based on two independent DFB lasers and PMLLD, where both coherent and incoherent receivers have been used. The generation of intensity noise and its impact close to beat note at mm-wave frequency have been demonstrated and investigated, while the phase noise results are provided as well for comparison. For measuring the real RIN_{beat} contribution, the frequency response of the system has been measured and removed. The experimental results confirm that RIN_{beat} close to the mm-wave carrier is directly generated from the initial RIN_{ini} at low frequency whatever the photonic generation process is and is clearly distinct from phase noise of the beat signal. It is also shown that, due to heterodyning, the RIN_{beat} level can be higher than the RIN_{ini} by a factor equal to the ratio between mode power. The models of classic definition of RIN laser RIN_{ini} and RIN generated close to the beat note RIN_{beat} are presented and agree very well with the experimental measurements. These results are independent from how the optical modes are generated, so they can directly be transposed to any kind of optical process for beat note frequency generation.

The EVM results have been demonstrated using the 60 GHz wireless transmission system to meet the 60 GHz communication standards, and the impairment of intensity noise is examined on the RoF performance.

Acknowledgment

The authors wish to thank Nicolas Corrao for his a valuable discussion, and we are thankful for the III-V lab, a joint laboratory of “Alcatel Lucent Bell Labs”, “Thales Research & Technology”, and “CEA-LETI”, Palaiseau, France, for providing the PMLLD chip.

References

[1] T. Kleine-Ostmann and T. Nagatsuma, “A review on terahertz communications research” *J. Infrared Millimeter Terahertz Waves*, vol. 32, pp. 143-171, Feb. 2011.

[2] N. Guo, R. C. Qiu, S. S. Mo, and K. Takahashi, “60 GHz millimeter-wave radio: principle, technology and new results” *Eurasip J. Wireless Communication Networks*, P. 8, 2007.

[3] Su-Khiong Yong, P. Xia, and A. Valdes-Garcia, “60 GHz technology for Gbps WLAN and WPAN: from theory to practice” *John Wiley and Sons*, 2011.

[4] P. Smulders, “Exploiting the 60 GHz band for local wireless multimedia access: prospects and future directions” *Communications Magazine, IEEE*, vol. 40, no. 1, pp. 140147, 2002.

[5] A. El Oualkadi, “Trends and challenges in CMOS design for emerging 60 GHz WPAN applications” *Advanced Trends in Wireless Communications*, Rijeka, Croatia: In Tech, Feb. 2011.

[6] C. Mann, “Practical challenges for the commercialization of terahertz electronics” *Proc. IEEE Int. Microw. Symp.*, pp 1705-1708, Jun. 2007.

[7] Z. Jia et al, “Key enabling technologies for optical-wireless networks: opticzl millimeter-wave generation, wavelength reuse, and architecture” *J. Lightw. Technol.*, vol. 25, no. 11, pp. 3452-3471, Nov. 2007.

[8] A. Stohr et al, “60 GHz radio-over-fiber technologies for broadband wireless services” *OSA J. Optical Networking*, vol. 8, no. 5, pp. 471-487, May 2009.

[9] F. Brendel et al, “Low-cost analog fiber optic links for in-house distribution of millimeter-wave signals” *International Journal of Microwave and Wireless Technologies*, pp. 231-236, Apr. 2011.

[10] L. A. Johansson, and A. J. Seeds, “Generation and transmission of millimeter-wave data modulated optical signals using an optical injection phase-lock loop” *J. Lightw. Technol.*, 21 (2), pp. 511-520, Feb. 2003.

[11] F. Van Dijk et al, “Monolithic dual wavelength DFB lasers for narrow linewidth heterodyne beat-note generation” *IEEE International Topical Meeting on Microwave Photonics 2011*, pp. 73-76, 18-21, Oct. 2011.

[12] J. Poette, P. Besnard, L. Bramerie, and J. C. Simon, “Highly-sensitive measurement technique of relative intensity noise and laser characterization” *Fluctuation and Noise Letter*, vol. 8, n. 1, pp. 81-86, Mar. 2008.

[13] H. Hallak Elwan, R. Khayatzedeh, J. Poette, and B. Cabon, “Relative intensity noise in optical heterodyning applied to millimeter wave systems” *IEEE International Topical Meeting on Microwave Photonics, MWP 2015, Paphos, Cyprus*, Oct. 26-29, DOI: 10.1109/MWP.2015.7356690, pp. 1-4, 2015.

[14] R. Khayatzadeh, J. Poette, and B. Cabon, “Impact of phase noise in 60 GHz radio-over-fiber communication system based on passively mode locked laser” *IEEE J. Lightw. Technol.*, vol. 32, no. 20, pp. 35293535, May 2014.

[15] R. Khayatzadeh, H. Hallak Elwan, J. Poette, and B. Cabon, “Impact of amplitude noise in millimeter-wave radio-over-fiber systems” *IEEE J. Lightw. Technol.*, vol. 33, no. 13, pp. 2913-2919, July 2015.

[16] R. Khayatzedeh,H. Hallak Elwan, J. Poette, and B. Cabon, “100 GHz RoF System Based on Two Free Running Lasers and Non-coherent Receiver” *IEEE International Topical Meeting on Microwave Photonics, MWP 2015, Paphos, Cyprus*, Oct. 26-29, DOI: 10.1109/MWP.2015.7356689, pp. 1-4, 2015.

[17] R. Khayatzadeh, H. Rzaigui, J. Poette, and B. Cabon, “Accurate millimeter-wave laser phase noise measurement technique” *IEEE Photonics Technology Letters*, vol. 25, no. 13, July 2013.

[18] http://www.ecma-international.org/publications/standards/Ecma387.htm

[19] https://standards.ieee.org/findstds/standard/802.15.3c-2009.html

[20] Govind P. Agrawal, “Optical transmitters” in “Fiber-optic communication systems” *John Wiley & Sons*, 3rd ed., 2002.

[21] Agilent E8257D PSG Microwave Analog Signal Generator Datasheet, Agilent Technol, Santa Clara, Ca, USA, 2012.

Hamza Hallak Elwan received the B.Sc. degree in electronics and communications engineering from Aleppo University, Aleppo, Syria, in 2010. He received the Master degree in electronics engineering and the Engineer Diploma in communications system engineering in a double degree program from Politecnico di Torino, Torino, Italy, and Institut Polytechnique de Grenoble (Grenoble-INP) Ensimag, Grenoble, France, in 2014. He is currently working toward the Ph.D. degree at IMEP-LAHC Laboratory and Grenoble-INP. His research fields are microwave-photonics, radio-over-fiber, and optical systems.

Ramin Khayatzadeh received the B.Sc. degree in electrical engineering in 2010 from Shiraz University, Shiraz, Iran, and the M.Sc. degree in electronics engineering and Dipl. Ing. degree in communication system engineering in a double degree program in 2012 from the Polytechnic of Turin, Turin, Italy, and French engineering school ENSIMAG, respectively. He is currently working toward the Ph.D. degree at IMEP-LAHC Laboratory, National Polytechnics Institute of Grenoble, Grenoble, France. His main research interests are terahertz communication systems, radio-over-fiber and microwave-photonics technology.

Julien Poette received, in 2002, an Engineer Diploma from the French engineering school ENSSAT (National School for Applied Science and Technologies), Lannion, France, with a specialization in opto-electronics and a Research Master degree in science and techniques of telecommunication. He received the Ph.D. degree in physics in 2005 from Rennes 1 University, Rennes, France. Since 2008, he joined the IMEP-LAHC Laboratory as an Associate Professor and is currently an Associate Professor at Grenoble-INP (National Polytechnics Institute of Grenoble), Grenoble, France.

Beatrice Cabon received the Ph.D. degree from the Institut Polytechnique Grenoble (Grenoble-INP), Grenoble, France, in 1986, and has been Professor from 1989. She is Head since 1993 of a research group on microwave-photonics techniques at IMEP-LAHC, Institute for Microelectronics, Electromagnetism and Photonics laboratory, Grenoble. From 1998 to 2008, she has been also coordinator of the club optics and microwaves of the French Optical Society. She also coordinated two European projects Networks of Excellence funded by the European commission, FP6-IST-2001-32786 NEFERTITI (20022005) and FP6-IST-26592 ISIS (20062009). Her research interests include microwave photonics, photonic-microwave signal processing, and optical links for high bit rate signals. She has authored or coauthored more than 250 technical publications and is the editor of five books in these areas.